Development of an Integrated Thrust Vectoring System for Nozzle-Augmented Electric Ducted Fans

Emily Yang*
Tennessee Technological University, Cookeville, TN, 38505

Bruce Jo†
Tennessee Technological University, Cookeville, TN, 38505

Emerging research demonstrates that electric ducted fans (EDFs) significantly outperform open rotors in terms of thrust generation and power efficiency. When adopted as the main propulsors in a distributed electric propulsion (DEP) configuration, EDFs also have the potential to simplify aircraft design while delivering superior controllability. This study details the development of a thrust vectoring mechanism for a nozzle-augmented EDF. The EDF-nozzle combination serves as the main propulsion unit of a vertical take-off and landing (VTOL) capable unmanned aerial vehicle (UAV) under development. To achieve thrust vectoring, three actuated airfoil-shaped flaps with rubber lining are integrated into the nozzle and deployed using two servo motors mounted on either side of the nozzle. Controlled through pulse width modulation (PWM), the servos uniformly transition the flaps from a stowed position (0°) for maximum horizontal thrust to a fully deployed state (90°) for maximum lift. Initial experimentation results demonstrate a thrust vectoring efficiency of 90.1%. This research addresses critical gaps in existing literature on the mechanical design and digital control of thrust vectoring mechanisms for EDFs and UAVs.

I. Introduction

A. Motivation and background

The global acceleration towards rapid urbanization has catalyzed the development of vertical takeoff and landing (VTOL) aircraft. These platforms are uniquely suited to infrastructure-packed and population-dense environments due to their runway independence and operational versatility. However, traditional VTOL configurations – including open-rotor, tiltrotor, jet-powered, and hybrid systems – face significant bottlenecks. They are often constrained by high mechanical complexity and limited energy density, which together restrict their operational endurance and payload capacity [1]. Consequently, current research is focused on simplifying control mechanisms, optimizing energy use, and perfecting the transition from hover to cruise flight [2].

A pivotal shift in addressing these limitations is the implementation of distributed electric propulsion (DEP). By decoupling the power source from propulsors, DEP replaces the traditional single-engine configuration with a synergetic array of propulsors distributed across the airframe. This flexibility enables configurations that yield superior thrust-to-weight ratios, reduced noise pollution, and dynamic control. A prominent iteration of this concept is turboelectric distributed propulsion, where a gas turbine drives a separate electric generator to power multiple distributed fans. This allows the turbine and fans to operate at independent, optimal speeds, significantly enhancing controllability and, when integrated into VTOL airframes, has been shown to increase cruise velocities [3]. Furthermore, in conventional takeoff and landing (CTOL) and short takeoff and landing (STOL) applications, distributing small propellers along the leading edge of the wing and larger cruise propellers at the wingtips reduces both wing area and drag [4]. Ultimately, DEP's compatibility with a wide range of airframes makes it a versatile solution for engine configurations.

Within the DEP framework, electric ducted fans (EDFs) have emerged as the optimal propulsor for urban aerial

*Undergraduate Student, Department of Mechanical Engineering, AIAA Student Member 1924220
† Associate Professor, Department of Mechanical Engineering, AIAA Member

mobility (UAM). Compared to open rotors, EDFs provide significantly higher static thrust, greater controllability, and enhanced safety by shielding rotating parts. Furthermore, the ducting provides an acoustic shroud that reduces noise pollution, a critical advantage in population-dense environments [5]. Recognizing the advantages, fully electric tilted-ducted fans based on Bell Textron's Nexus 6HX were integrated into an electric VTOL (eVTOL) to reduce traffic congestion and carbon emissions [6]. Current research seeks to maximize these advantages through configuration-specific optimization. For instance, the optimization of a ducted-fan wing unit on a DEP eVTOL aircraft has adopted a canard configuration, achieving a maximum speed of 720 km/h, hovering efficiency of 76.3%, and a cruise-to-drag ratio of 10.7 [7]. These benchmarks, along with various studies on EDF-integrated VTOLs, demonstrate the vast potential for EDFs to redefine aircraft design and efficiency.

To dynamically modulate the orientation and magnitude of propulsive forces, VTOL aircraft frequently employ specialized thrust vectoring mechanisms. A common approach is rotor disc tilting, wherein the entire propulsor unit is articulated along the pitch and yaw axes to manipulate the resultant thrust vector directly [8]. Alternatively, recent advancements in airflow vector estimation allow tilt-wing eVTOLs to control aerodynamic forces by calculating the interaction between the wing and propulsor [9]. A comprehensive review of thrust vectoring technologies identifies distinct trade-offs across current methodologies: mechanical systems offer high-precision control but add structural burden, fluidic systems improve response speed but result in thrust loss, and DEP system improves hovering capabilities compared to traditional open rotors [10].

B. Research Objective and Scope

While many studies have validated the aerodynamic effects of thrust vectoring in VTOL applications, there remains a notable gap in the availability of explicit, open-access documentation regarding their mechanical design and control. This paper aims to bridge that gap by providing a detailed design framework for a newly proposed thrust vectoring system for a nozzle-augmented EDF in a VTOL aircraft. The design focuses on simplifying the propulsion system through an alternative method for the hover-to-cruise transition. To provide an in-depth description of the proposed mechanism, this paper focuses primarily on the mechanical design and system layout rather than on extensive aerodynamic performance metrics.

II. Methodology

A. Propulsion Unit

The propulsion unit consists of a high-capacity Lithium-Polymer (LiPo) battery pack that powers a specialized electronic speed controller (ESC). Controlled via pulse-width modulation (PWM) from an Arduino Mega 2560 microcontroller, the ESC modulates the electrical frequency and current delivered to the driving motor, thereby regulating the EDF's rotational speed. Each component was selected for its ability to meet the high-power demands of eVTOL applications.

The ZTW Skyhawk 160A High-Voltage ESC was selected as the motor's power regulator. It utilizes a high-performance 32-bit M4 microprocessor running at 170 MHz to ensure uniform throttle control and rapid motor response. This unit supports an input voltage range of 65 to 145 LiPo and is rated for a continuous current of 160 A, with burst capabilities up to 180 A. It integrates an adjustable switch-mode battery elimination circuit (SBEC) capable of delivering 10 A at three different voltage levels. The ESC utilizes MOSFET technology for low heat generation and includes multiple protection protocols, including abnormal power-on voltage, temperature, throttle signal loss, and over-current protection. The ESC is encased in a specialized case that includes a fan guard to optimize heat dissipation during operation.

The motor used is the HET Typhoon 800 73 590KV Brushless DC (BLDC) motor. It is engineered for 100-120 mm EDF units. Featuring an 8-pole design and a 50 mm diameter, the motor is designed for high power output, supporting up to 7040 W. It is compatible with 12S or 14S Li-Po battery configurations, with recommended ESC ratings of 150 A for 12S and 130 A for 14S setups. The motor measures 73 mm in length, with an 8 mm shaft diameter, and weighs 495 g.

The above units ultimately drive the E-Jets Jetfan 120mm Pro EDF unit. It is an 11-blade modular rotor designed to deliver a smooth turbine-like "whooshing" sound profile by minimizing high-pitch frequencies. The unit features an aluminum inner housing and an aluminum hub to facilitate motor cooling, with an all-carbon housing and six carbon fiber stators. It has an outer housing diameter of 123 mm, an inner diameter of 121 mm, and a total housing length of 80 mm. The aerodynamic design of this EDF improves suction performance even with small air inlets.

B. Nozzle Design

To facilitate the transition between vertical lift and horizontal cruise, a custom thrust-vectoring nozzle was developed using computer-aided design (CAD) software and fabricated using additive manufacturing. The assembly was 3D-printed using Polymaker PolyLite PLA Pro, a high-performance filament engineered for professional-grade mechanical properties. This material exhibits a high Young's Modulus of roughly 2932 MPa and tensile strength of nearly 50 MPa. These metrics ensure the necessary structural rigidity to withstand the thrust and internal pressures exerted by the 120 mm EDF without deforming. However, the PolyLite PLA's glass transition temperature of 62° would not be able to withstand the heat generated by the HET motor during long runs. Subsequently, testing on the nozzle's performance is done only for a short duration.

The nozzle's geometry is characterized by a cylindrical shell that securely frames the EDF exit diameter. The structure morphs from a circular profile at the intake to a rectangular profile at the exhaust. This transition is designed to optimize a path for the internal vectoring flaps. When viewed laterally, the nozzle's profile resembles an inverted right trapezoid: the vertical side serves as the primary interface for thrust generation, while the exhaust is directed towards the angled, non-parallel trailing edge. A visual of the nozzle is provided in Figure 1.

Figure 1. Custom-engineered nozzle

For precise thrust redirection, three airfoil-shaped flaps are positioned horizontally within the nozzle's rectangular exhaust section. These flaps are vertically equidistant and contained entirely within the trapezoidal volume of the outer shell. To optimize aerodynamic efficiency, each flap extends toward the internal walls without making direct contact; instead, rubber tape is applied to the lateral edges of each flap. This creates a low-friction seal that prevents pressure leakage while allowing the surfaces to slide smoothly against the nozzle walls during linear actuation. The control logic of the surfaces is divided into two parts: the topmost flap articulates independently, while the lower two flaps are mechanically conjoined to function as a singular unit. Flap orientation within the outer shell is demonstrated in Figure 2.

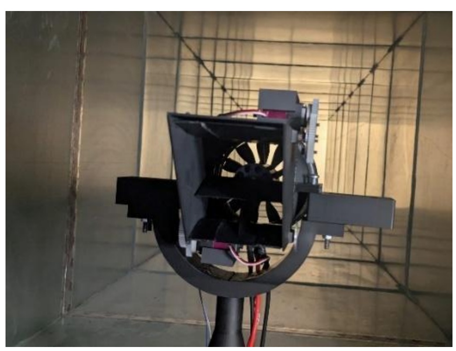

Figure 2. Flap orientation

At the axis of rotation for each flap unit, a D-shaped bore is utilized to interface with a corresponding D-shaped drive shaft. This configuration provides a simplistic yet robust mechanical coupling, ensuring that rotational torque is uniformly distributed across the flap surface without the risk of slipping associated with round shafts. Aluminum was the selected material for the drive shafts due to its high tensile strength compared to a small cross-sectional area. This allows deployed flaps to remain rigid while reducing flow blockage within the exhaust stream.

The actuation is powered by two high-torque servos, each capable of delivering 160 kg·cm of torque. This substantial torque is necessary to overcome the aerodynamic resistance acting on the flaps during high-throttle operations. The servos are mounted in a custom-engineered casing: one is positioned on the upper exterior of the nozzle, while the second is located on the opposing lateral wall near the base. A 48-tooth hub mount gear is fixed to each servo output, driving a 60-tooth gear secured to the aluminum drive shaft. This configuration establishes a 4:5

gear ratio. Figure 3 provides a demonstration of the orientation of the servos and gear connections.

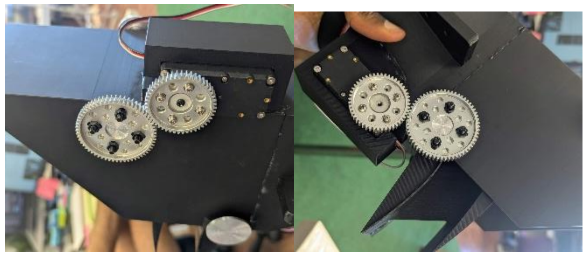

Figure 3. Servo and gear configurations

C. Servo Command

To ensure maximum precision and minimize jitter in the actuation of the 160 kg·cm servos, the Arduino Mega 2560 (ATmega2560) is configured to operate via PWM rather than standard libraries. Each servo is assigned to a discrete 16-bit hardware timer (timers 1 and 5, respectively) to prevent resource contention. The timer control registers (TCCRnA/B) are reset to initialize a non-inverting, Fast PWM (mode 14), which utilizes the ICRn register as the TOP value to define the PWM period. With the microcontroller's system clock running at 16 MHz and a prescaler of 8, the clock frequency is effectively reduced to 2 MHz. To achieve a standard 50 Hz frequency (20 ms period) required for analog servo communication, the TOP value is calculated to be 39,999.

The target flap angles (0° to 180°) are mapped to their corresponding pulse widths, typically ranging from 500 µs to 2500 µs. Because the servos are mounted in a mirrored configuration on the nozzle housing, their rotational directions are inverted relative to the flap's axis of rotation. To compensate for this, the software implements an inverse mapping logic: while the primary servo maps 0°-180° to 500-2500 µs, the auxiliary servo maps the same angular range to 2500-500 µs. While mechanical tolerances and instrumental inaccuracies can lead to slight deviations in the pulse width range, the 4:5 gear ratio provides a mechanical buffer. This allows the ATmega2560 to calibrate the mapping specifically to the final flap orientation rather than the raw output of the servo.

The home position is defined at 0°, corresponding to a horizontal flap orientation, while the maximum sweeping angle is set to 90° for vertical thrust redirection. The transition is managed through an incremental iterative method using a conditional loop: if the current indexed angle is ≥ 90°, the value is decremented by 1° per cycle. Conversely, if the angle ≤ 0°, it is incremented by 1°. This ensures a continuous, controlled sweep across the 90-degree vectoring range, facilitating a smooth transition between hover and cruise flight while protecting the actuation system from excessive torque spikes.

D. Experimental Procedure

To characterize the aerodynamic performance of the thrust-vectoring assembly, testing was conducted by automating servo sweeps across the full deflection range of 0° to 90°, with a subsequent return to the 0° home position via the ATMega2560 microcontroller. The nozzle flaps were deployed in linear angular increments, with sufficient dwell times at each position to mitigate transient effects and ensure both thermal and aerodynamic stability. For each test sequence, the motor throttle was maintained at a constant PWM signal, ranging from 1100 µs to 2000 µs. Upon completion of a sweep, the throttle was incremented for the subsequent sequence. This experimentation resulted in 4,800 measurements, sampled at 10 Hz, used to quantify the nozzle design's efficiency.

III. Results and Discussion

The primary metric for evaluating the nozzle-augmented EDF was the thrust efficiency during the vectoring process. Raw output of the Jetfan 120 Pro is compared against the output after integrating the 3D printed nozzle assembly. Experimental results yielded a thrust efficiency of 90.1%. This high efficiency is attributed mainly to the maintenance of an aerodynamic profile in the internal flaps.

Specific power, the electrical power required to generate a unit of thrust (W/N), was analyzed in this study to measure power efficiency. The average specific power collected through the experimentation was 64.14 W/N from a range of 16.77 W/N to 141.46 W/N. Minimum specific power consumption occurred during moderate throttle (1400 µs – 1600 µs) and minimal deflection (0° - 15°), while maximum power consumption occurred at high deflection (75° - 90°). This suggests that the HET motor and Jetfan EDF operate at their peak efficiency when the internal flow path is least obstructed.

A significant point of analysis in this study was the translation of motion from the servos to the airfoil flaps. While the system achieved notable outcomes in thrust redirection, quantifying the absolute accuracy of the gear connection presented a notable limitation. This limitation could potentially be addressed by using rotary encoders to measure discrepancies in the resultant angle and the intended angle.

Acknowledgments

I am most indebted to the graduate students, Jakob Coats and Oluwadara Odukoya, who contributed to the design and data collection of this paper's topic, as well as the revision of this paper itself. Additionally, I thank Dr. Bruce Jo for providing me with not only this research opportunity but also for recommending my involvement in various conferences.

References

[1] Yuan, D., "The Overview of Vertical Take-Off and Landing Technology," *Applied and Computational Engineering*, 93, 2024, pp. 40-44. https://doi.org/10.54254/2755-2721/93/2024BJ0069.

[2] Bridgelall, R., "Aircraft Innovation Trends Enabling Advanced Air Mobility," *Inventions*, 9, 84, 2024. https://doi.org/10.3390/inventions9040084.

[3] Kim, H. D., Perry, A. T., Ansell, P. J., "A Review of Distributed Electric Propulsion Concepts for Air Vehicle Technology," *2018 AIAA/IEEE Electric Aircraft Technologies Symposium*, AIAA Paper 2018-4998. https://doi.org/10.2514/6.2018-4998.

[4] Borer, N. K., Patterson, M. D., Viken, J. K., Moore, M. D., Bevirt, J., Stoll, A. M., Gibson, A. R., "Design and Performance of the NASA SCEPTOR Distributed Electric Propulsion Flight Demonstrator," *16th AIAA Aviation Technology, Integration, and Operations Conference*, AIAA Paper 2016-3920, https://doi.org/10.2514/6.2016-3920.

[5] Chou, T., Ying, Q., Qian, Y., Zhuge, W., Zhang, Y., "Study on Overall Design of a Vertical Take-Off and Landing Unmanned Aerial Vehicle Powered by Electric Ducted Fans," *Proceedings of the ASME 2021 Fluids Engineering Division Summer Meeting*. Vol. 2, No. FEDSM2021-65556, 2021. https://doi.org/10.1115/FEDSM2021-65556.

[6] Lee S. G., Ko B. S., Ahn S. H., Hwang H. Y., "Initial Sizing of a Tilt Ducted Fan Type eVTOL for Urban Air Mobility," *J. Korean Soc. Aviat. Aeronaut*, Vol. 29, No. 3, 2021, pp. 52-65. https://doi.org/10.12985/ksaa.2021.29.3.052.

[7] Ma, T., Wang, X., Qiao, N., Zhang, Z., Fu, J., and Bao, M., "A Conceptual Design and Optimization Approach for Distributed Electric Propulsion eVTOL Aircraft Based on Ducted-Fan Wing Unit," *Aerospace*, Vol. 9, No. 11, 2022, Art. 690. https://doi.org/10.3390/aerospace9110690.

[8] Amoozgar, M., Hall, M., Dimitriadis, G., Cooper, J. E., "The Effect of Thrust Vectoring on Aeroelastic Stability of Electric Aircraft, *Aeroelastic Problems for Electric-Aircraft and Unmanned Aerial Vehicles*, AIAA 2024-2044. https://doi.org/10.2514/6.2024-2044.

[9] Yokota, K., and Fujimoto, H., "Aerodynamic Force Control for Tilt-Wing eVTOL Using Airflow Vector Estimation," IEEE Transactions on Transportation Electrification, Vol. 8, No. 4, 2022, pp. 4163–4172. https://doi.org/10.1109/TTE.2022.3162946.

[10] Luo, Y., Cui, B., and Zhang, H., "Review of Thrust Vectoring Technology Applications in Unmanned Aerial Vehicles," Drones, Vol. 9, No. 10, Art. 689, 2025. https://doi.org/10.3390/drones9100689.